

## Microstructure and Mechanical Properties of Die Cast Magnesium-Aluminum-Tin Alloys

A.A. Luo<sup>1</sup>, P. Fu<sup>2</sup>, X. Zeng<sup>2</sup>, L. Peng<sup>2</sup>, B. Hu<sup>3</sup>, A.K. Sachdev<sup>1</sup>

<sup>1</sup>General Motors Global Research and Development, Warren, MI 48090, USA

<sup>2</sup>Shanghai Jiao Tong University, Shanghai, China

<sup>3</sup>General Motors China Science Laboratory, Shanghai, China

Keywords: Magnesium alloys, alloy development, computational alloy design, microstructure

### Abstract

Mg-Al-Sn alloy system offers good combination of strength, ductility, castability and corrosion resistance for potential automotive structural applications. This report summarizes the microstructure and mechanical properties of two Mg-Al-Sn alloys, AT72 (Mg-7Al-2Sn<sup>1</sup>) and AT96 (Mg-9Al-6Sn), prepared using high pressure die casting process. The microstructure of as-cast Mg-Al-Sn alloys was investigated using computational thermodynamics modeling and experimental techniques. Both alloys show improved mechanical properties and excellent die castability compared with the conventional AZ91 (Mg-9Al-1Zn) and AM50 (Mg-5Al-0.3Mn) alloys. The AT72 alloy is currently used in developing large thin-wall die cast door inners and cast magnesium wheels.

### Introduction

Magnesium is the lightest metal available for reducing the weight of automotive structural subsystems for improved fuel economy. A unique characteristic of magnesium, in addition to its low density, is its extreme fluidity, which enables it to be die cast into shapes that are thinner and more complex than can be obtained with aluminum. There are currently two major magnesium alloy systems for high pressure die casting (HPDC) applications; Mg-Al-Zn (AZ) and Mg-Al-Mn (AM): both have limited mechanical properties [1]. AZ91 (Mg-9Al-1Zn) alloy has moderate strength but low ductility, and is generally used for non-structural parts like brackets, covers, cases and housings that are strength dominated and exposed to ambient temperatures. For semi-structural applications such as instrument panels, steering systems and radiator supports, where crashworthiness is important, AM50 (Mg-5Al-0.3Mn) or AM60 (Mg-6Al-0.3Mn) are used due to their higher ductility (10-15% elongation). However, the yield strength of AM50/60 alloy is too low for many critical automotive structural applications.

The major strengthening phase in Mg-Al based alloys is Mg<sub>17</sub>Al<sub>12</sub> ( $\beta$  phase), which is resistant to dislocation shearing but its distribution is relatively coarse, presumably because of the relatively high diffusion rate of Al atoms in the solid matrix of magnesium and a possibly high concentration of vacancies in the  $\alpha$ -Mg matrix [2]. A recent development at GM [3] showed improved mechanical properties of Mg-Al-Sn ternary alloys, due to the dual strengthening phases of Mg<sub>17</sub>Al<sub>12</sub> and Mg<sub>2</sub>Sn. A further study [4] using computational thermodynamics coupled with experimental validation has suggested two Mg-Al-Sn alloys, AT72 (Mg-7Al-2Sn) and AT96 (Mg-9Al-6Sn), which offer good combinations of strength and ductility.

This paper summarizes the microstructure and mechanical properties of the two Mg-Al-Sn alloys (AT72 and AT96), prepared using high pressure die casting process. The microstructure of the as-cast alloys was investigated using computational thermodynamics modeling and experimental techniques.

### CALPHAD Modeling and Experimental Procedure

#### CALPHAD and Heat Treatments

The CALPHAD (CALculation of PhAse Diagrams) approach based on computational thermodynamics, described in details in an earlier publication [5], was used to calculate the phase equilibrium of the Mg-Al-Sn alloy system and the two alloys in this study. The calculations were carried out using Pandat code developed by CompuTherm (Madison, WI) [6] and the extensive thermodynamic database for Mg-based alloys (PanMg) developed by Clausthal University of Technology (Clausthal, Germany) [7].

#### Alloy Preparation and Die Casting

The AT72 and AT96 alloys were prepared using AM60B (base alloy), pure Al and pure Sn ingots. The chemical compositions of the alloys are listed in Table 1. Both alloys were die cast into an experimental bracket casting with a shot weight of about 1 kg in magnesium (Fig. 1) on a 500 T die casting machine at a vacuum level of 0.2 bar. Due to the different liquidus temperatures reported for the two alloys, 610°C for AT72 and 590°C for AT96 [3], the alloys were die cast at 700°C and 680°C, respectively. About 200 shots were made for each alloy, and both alloys showed excellent castability with no visible casting defects when the casting trails reached the steady state of operation.

Table 1. Nominal alloy composition and ICP analysis results

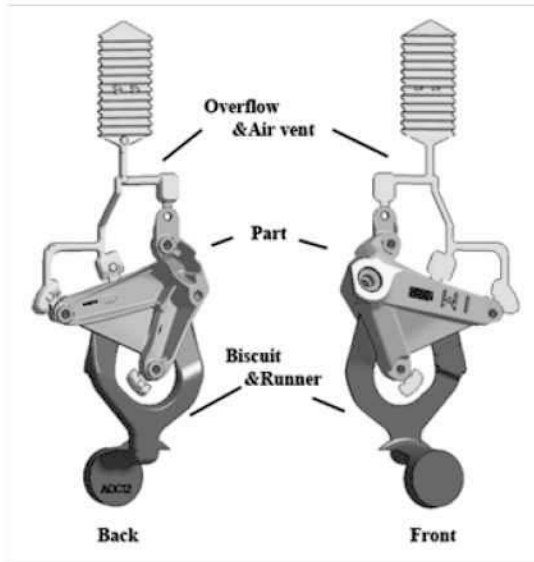
Alloy	Nominal composition	Al	Sn	Zn	Mn	Fe	Ni	Cu
AT72	Mg-7Al-2Sn	7.3	3.1	<0.01	0.01	0.01	<0.003	<0.003
AT96	Mg-9Al-6Sn	9.1	6.4	<0.01	0.01	0.01	<0.003	<0.003

#### Mechanical Testing and Microstructural Analyses

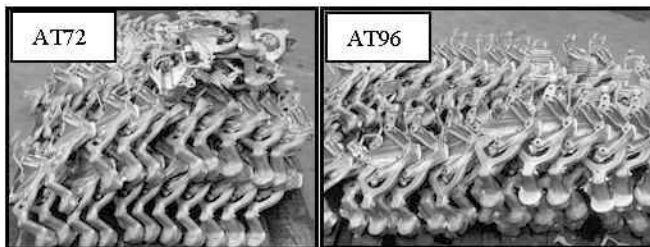
ASTM subsize tensile bars of 25 mm gage length and 7.6 mm width were machined from the flat sections of the castings (as-cast and heat-treated) of about 4 mm thickness with the casting surfaces maintained. Tensile testing was carried out at room temperature according to ASTM E21-92 procedures at an initial strain rate of 0.001 s<sup>-1</sup>. For each alloy, at least three specimens were tested and the average properties reported. Specimens for microstructural analyses were sectioned from the center of the tensile bars, and then polished and etched according to standard metallographic procedures. The microstructure of the alloy specimens was analyzed using a Nikon Epiphot optical microscope and a Cameca SX100 Electron Probe Microanalyzer (EPMA). Quantitative image analysis was used to measure the

<sup>1</sup> All compositions in wt.% except otherwise stated.

area fractions of the second phases from the backscattered electron images of the as-cast alloys.



(a) Die design



(b) AT alloy castings



(c) A complete casting with gating system

Fig. 1. Experimental bracket casting with a shot weight of 1.04 kg in magnesium.

## Results and Discussion

### Solidification Sequence and Microstructure

Fig. 2 shows the calculated liquidus projection of the Mg-Al-Sn system in the Mg-rich corner, using the CALPHAD approach. No stable ternary phase was discovered, and no ternary solubility of the binary intermetallic phases was found in this calculation, which is consistent with a previous study [9]. Two binary phases,  $Mg_2Sn$  and  $Mg_{17}Al_{12}$ , are important to this alloy system: the  $Mg_2Sn$  phase is reported to provide significant strengthening [3], while the  $Mg_{17}Al_{12}$  phase improves strength [9], corrosion and castability [10], but reduces ductility and creep resistance [11].

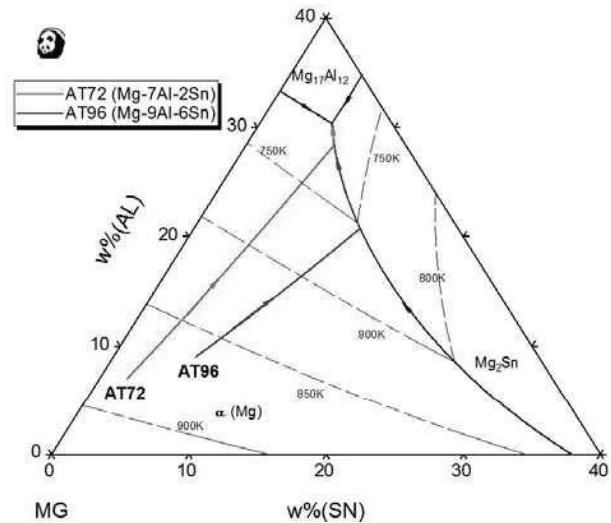


Fig. 2. Calculated Mg-Al-Sn liquidus projection and the solidification paths of AT72 and AT96 alloys.

Fig. 3 shows the calculated solidification sequence of AT72 & AT96 alloys based on the Scheil model, assuming complete mixing in the liquid but no diffusion in the solid. The solidification paths for both alloys are summarized as follows:

- 1) Nucleation of primary magnesium (from 610°C for AT72 and 590°C for AT96):  $L \rightarrow L + \alpha\text{-Mg}$
- 2) Binary eutectic reaction (from 441°C for AT72 and 479°C for AT96):  $L \rightarrow L + \alpha\text{-Mg} + Mg_2Sn$
- 3) Ternary eutectic reaction (430°C):  $L \rightarrow L + \alpha\text{-Mg} + Mg_2Sn + Mg_{17}Al_{12}$

The final microstructure of AT72 and AT96 alloys, as shown in Fig. 4, consists of very fine  $\alpha\text{-Mg}$  dendrites surrounded by eutectic intermetallic phases. Further identification of the eutectic phases is shown in the EPMA images along with the element maps of Al, Sn and Mg, Figs. 5 and 6. It is clear that the fine bright particles of 1-2  $\mu\text{m}$  size containing Mg and Sn, are  $Mg_2Sn$ , while the gray eutectic network along the grain boundaries are  $Mg_{17}Al_{12}$ .

Table 2 compares the Scheil simulation results and the experimental measurements of the second phase contents of Mg-Al-Sn alloys, which shows a reasonably good agreement between the experimental and simulation results for  $Mg_{17}Al_{12}$  and  $Mg_2Sn$  phases. The measured fractions are slightly lower (about 5% – 8%) than the Scheil simulation results due to the fact that the Scheil model does not consider diffusion in the solid, which affects solidification kinetics despite the high cooling rate in high-pressure die casting.

Table 2. Scheil simulation results and experimental measurements of the second phase contents of Mg-Al-Sn alloys

Alloy	$Mg_{17}Al_{12}$		$Mg_2Sn$	
	Calculated (volume %)	Measured (area %)	Calculated (volume %)	Measured (area %)
AT72 (Mg-7Al-2Sn)	7.3	6.78	0.5	0.46
AT96 (Mg-9Al-6Sn)	11.3	10.92	2.0	1.94

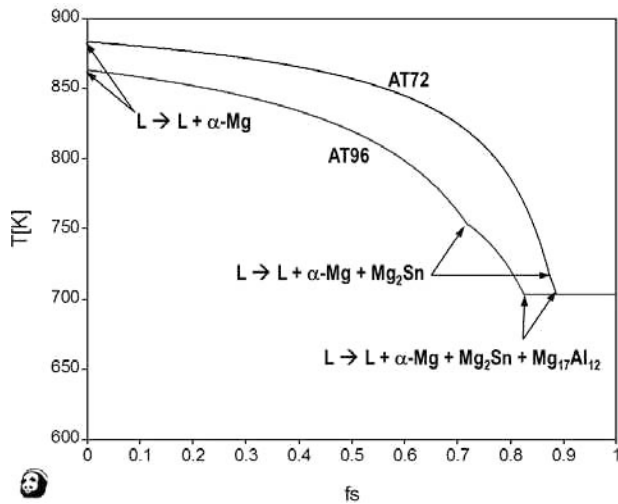


Fig. 3. Scheil simulation results of solidification sequence of AT72 and AT96 alloys.

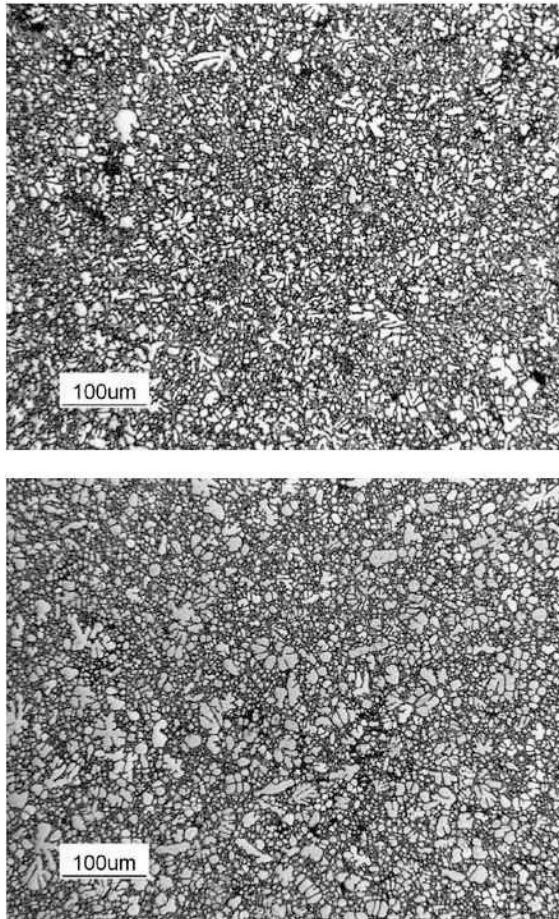


Fig. 4. Optical micrographs showing the as-cast microstructure of (a) AT72; and (b) AT96 alloys.

Mechanical Properties

Table 3 summarizes the mechanical properties of die cast AT72 and AT96 alloys compared with those of conventional die cast magnesium alloys (AZ91 and AM50). Compared with the AZ91 alloy, the AT72 and AT96 alloys show 5% and 26% higher yield

strength, respectively. While the high-strength AT96 alloy has 40% less ductility (elongation) than the AZ91 alloy, the AT72 alloy has more than doubled the elongation of AZ91. Compared with the AM50 alloy, the AT72 and AT96 alloys exhibited significantly more increases in yield strength, i.e., 37% and 63%, however, at considerable expenses in ductility. Overall, AT96 is a high-strength alloy with limited ductility, but the AT72 alloy offers more balanced increase in strength and ductility.

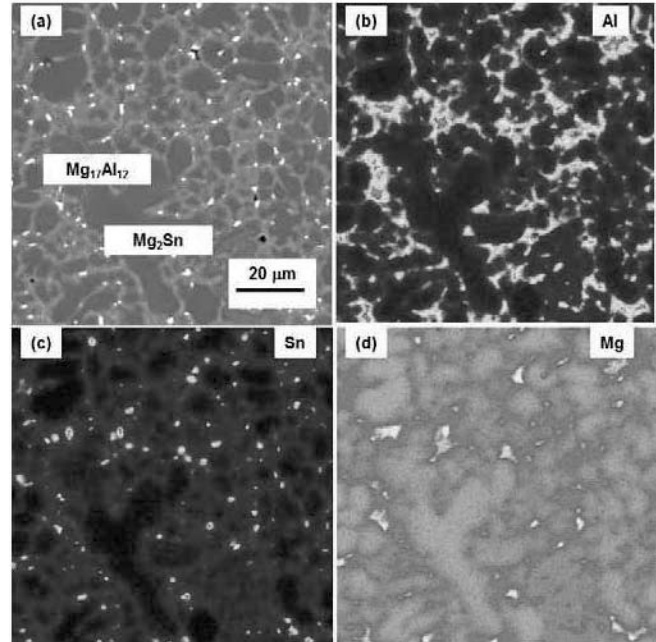


Fig. 5. Electron probe micro-analysis (EPMA) results showing the as-cast microstructure of AT72 alloy: (a) backscattered electron image; (b) Al map; (c) Sn map; and (d) Mg map.

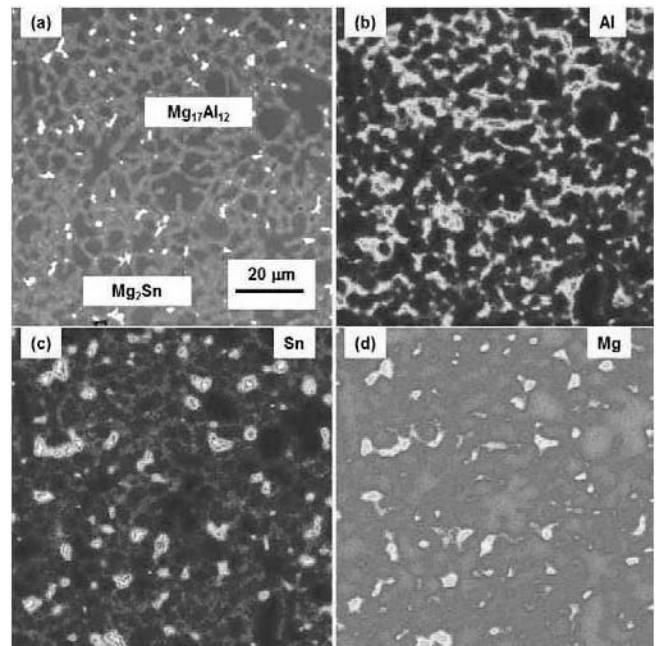


Fig. 6. Electron probe micro-analysis (EPMA) results showing the as-cast microstructure of AT96 alloy: (a) backscattered electron image; (b) Al map; (c) Sn map; and (d) Mg map.

Table 3. As-cast Mechanical properties of die cast alloys

Alloy	Yield Strength, MPa	Ultimate Tensile Strength, MPa	Elongation, %
AT72	158	251	6.3
AT96	189	216	1.8
AZ91	150	240	3
AM50	116	210	10

The reason for increased strengthening in Mg-Al-Sn alloys is due to the strengthening effects of both  $Mg_{17}Al_{12}$  and  $Mg_2Sn$  phases, while  $Mg_{17}Al_{12}$  is the only strengthening phase in Mg-Al binary alloys such as AZ91 and AM50. However, the higher volume fractions of  $Mg_{17}Al_{12}$  and  $Mg_2Sn$  phases in the AT96 alloy results in lower ductility compared to AT72 alloy, due to brittleness of both phases. From the morphology point of view, the  $Mg_2Sn$  is generally more rounded particles with small sizes than the  $Mg_{17}Al_{12}$  network. Therefore, it seems reasonable to assume that  $Mg_{17}Al_{12}$  phase is more detrimental to the ductility than the  $Mg_2Sn$  in the die casting microstructure. This is supported by the much higher ductility of AM50 alloy than AZ91 due to the higher Al content in the later alloy.

#### Castability

The castability of magnesium, i.e., the ease of casting with minimum defects, has been a subject of many publications [12-16]. Castability is generally influenced by a number of factors that are either alloy-dependent or process-dependent. Alloy-dependent parameters include feeding characteristics (i.e. fluidity), susceptibility to hot-tearing and cracking, freezing range, shrinkage and thermal properties (such as latent heat, heat capacity and thermal conductivity), while process-dependent factors are comprised of casting parameters (such as cooling rate and die surface condition) and die design considerations (geometry) [14]. In this study, the castability of Mg-Al-Sn alloys is discussed with the thermal physical properties that were calculated from the Scheil simulation, and compared with those of commercial alloys AM50 and AZ91 alloys (Table 4).

Table 4 compares the non-equilibrium (Scheil model) freezing range (the temperature difference between liquidus and solidus) of the AT72 and AT96 alloys with AM50 and AZ91 alloys. The calculated freezing range for the AM50 and AZ91 alloys agree very well with experimental measurements using differential scanning calorimetry (DSC) [17] and thermal analysis [18] techniques. It is generally agreed that alloys with wide freezing ranges are more difficult to cast, due to their strong tendency for non-uniform solidification [19]. Mg-Al based alloys with wide freezing ranges, such as AM50, are prone to micro-shrinkage, susceptible to hot-tearing [19], and less fluidity [13]. AZ91 alloy has a shorter freezing range compared to AM50, thus more castable than the AM50 alloy, as evident in several studies [13-15]. The freezing range of Mg-Al-Sn alloys becomes shorter with increasing Al and Sn contents, and both AT72 and AT96 alloys have shorter freezing range than that of AM50 alloy, indicating better castability than AM50, but similar to AZ91 alloy which is the most castable commercial magnesium alloy [18]. Another factor affecting the ability of molten metal filling the interdendritic regions is the amount of eutectic phases remaining in the last stage of solidification. Generally, alloys with more eutectic liquid such as AZ91 with 11% eutectic fraction have

better castability [18]. The AT72 and AT96 alloys have similar eutectic fractions (2 to 3 times higher than AM50) as that of AZ91, another indication of good castability of AT alloys.

Table 4. Scheil simulation results of die cast magnesium alloys

Alloy	Nominal Composition	Freezing Range, °C	Total Eutectic Fraction, vol.%	Total Latent Heat, J/mol
AZ91	Mg-9Al-1Zn	163	11.0	7637
AM50	Mg-5Al-0.3Mn	188	4.3	7866
AT72	Mg-7Al-2Sn	180	8.2	7528
AT96	Mg-9Al-6Sn	160	13.2	7387

The latent heat calculated from the Scheil simulation of the AT alloys is also compared with the AM50 and AZ91 alloys in Table 4. Generally, high latent heat can prolong solidification, thus, improves fluidity, and also enhances feeding to reduce micro-porosity and hot-tearing. However, the AZ91 alloy, and more castable than AM50 [13-15], has a lower latent heat than AM50. This is perhaps due to the shorter freezing range of the AZ91 alloy, which is a more important factor than latent heat [13]. It is interesting to note that the latent heat of both AT alloys is lower than that of AM50 or AZ91 alloy. From this study, both alloys show excellent die castability in the casting trial as shown in Fig. 1(b).

#### Conclusions

1. Compared with commercial AZ91 and AM50 alloys, both AT72 and AT96 alloys show improved yield strength. The AT96 is a high-strength alloy with limited ductility, while the AT72 alloy offers more balanced improvements in strength and ductility.
2. Computational thermodynamics modeling of phase equilibria in Mg-Al-Sn alloy system predict the formation of  $\alpha$ -Mg,  $Mg_{17}Al_{12}$  and  $Mg_2Sn$  phases in the solidification microstructure. This is validated by examining the microstructure of high-pressure die casting of two alloys, AT72 (Mg-7Al-2Sn) and AT96 (Mg-9Al-6Sn).
3. The Scheil simulation results and the experimental measurements of the second phase contents ( $Mg_{17}Al_{12}$  and  $Mg_2Sn$  phases) of Mg-Al-Sn alloys show a reasonably good agreement, indicating applicability of Scheil model in simulating the die casting microstructure.
4. The freezing range, total eutectic fraction and latent heat of AT72 and AT96 alloys calculated from thermodynamics modeling and the casting experiments confirm the excellent die castability of both Mg-Al-Sn alloys compared with commercial AZ91 and AM50 alloys.

#### Acknowledgments

This work was carried out as a collaborative research project supported by General Motors Global Research and Development (GM R&D), Warren, MI, USA, and Shanghai Jiao Tong

University (SJTU), Shanghai, China. The authors acknowledge Richard Waldo for carrying out EPMA analysis, Willie Dixon for optical metallography and Todd Meitzner for tensile testing.

### References

1. A.A. Luo, *International Materials Reviews*, 2004, 49, (1), 13-30.
2. J.-F. Nie, *Metallurgical and Materials Transactions A*, 2012, 43A, 3891-3939.
3. A.A. Luo and A.K. Sachdev, in *Magnesium Technology 2009*, eds. E.A. Nyberg, S.R. Agnew, N.R. Neelameggham and M.O. Pegguleryuz, TMS, Warrendale, PA, 2009, 437-443.
4. A.A. Luo, P. Fu, L. Peng, X. Kang, Z. Li, T. Zhu, *Metallurgical and Materials Transactions A*, 2012, 43A, 360-368.
5. A.A. Luo, R.K. Mishra, B.R. Powell, A.K. Sachdev, *Materials Science Forum*, 2012, 706-709, 69-82.
6. CompuTherm LLC: Pandat 8.0 - Phase Diagram Calculation Software for Multi-component Systems (CompuTherm LLC, Madison, WI, USA, 2008).
7. R. Schmid-Fetzer, A. Janz, J. Grobner and M. Ohno: *Advanced Eng. Mater*, 2005, 7, 1142.
8. E. Doernberg, A. Kozlov and R. Schmid-Fetzer, *Journal of Phase Equilibria and Diffusion*, 2007, 28, 523-535.
9. A.A. Luo and A.K. Sachdev: *International Journal of Metalcasting*, 2010, 4 (4), 51-58.
10. D. Sachdeva, S. Tiwari, S. Sundarraj and A.A. Luo, *Metallurgical and Materials Transactions B*, 2010, 41B, 1375-1383.
11. C.L. Mendis, C.J. Bettles, M.A. Gibson, C.R. Hutchinson, *Mater. Sci. Eng. A*, 2006, 435-436, 163-171.
12. B.R. Powell, A.A. Luo, B.L. Tiwari, and V. Rezhets: in *Magnesium Technology 2002*, ed., H.I. Kaplan, TMS, Warrendale, PA (2002), p. 123.
13. D. Argo, M. Pegguleryuz, P. Labelle, P. Vermette, R. Bouchard, M. Lefebvre: in *Magnesium Technology 2002*, ed., H.I. Kaplan, TMS, Warrendale, PA (2002), p. 87.
14. M.O. Pegguleryuz, P. Labelle, D. Argo, E. Baril: in *Magnesium Technology 2003*, ed., H.I. Kaplan, TMS, Warrendale, PA (2003), p. 201.
15. A.L. Bowles, Q. Han, J.A. Horton: in *Magnesium Technology 2005*, eds., N.R. Neelameggham, H.I. Kaplan, and B.R. Powell, TMS, Warrendale, PA (2005), p. 99.
16. S.S. Khan, N. Hort, I. Steinbach, S. Schmauder: in *Magnesium Technology 2008*, eds., M.O. Pegguleryuz, N.R. Neelameggham, R.S. Beals, E.A. Nyberg, TMS, Warrendale, PA (2008), p. 197.
17. D. Mirkovic, R. Schmid-Fetzer: *Metall Mater Trans A*, 2007, 38, 2575.
18. A. Luo: in *Proc. of the Third International Magnesium Conference*, Ed., G.W. Lorimer, The Institute of Materials, London, UK, 1996, 449.
19. ASM International: *Casting Design and performance*, ASM International, Materials Park, Materials Park, OH, 2009, 101.